energies

MDPI

Article

Performance Analysis of a Full Order Sensorless Control Adaptive Observer for Doubly-Fed Induction Generator in Grid Connected Operation

Gianluca Brando, Adolfo Dannier * and Ivan Spina

Department of Electrical Engineering and Information Technologies, University of Naples Federico II, Via Claudio 21, 80125 Napoli, Italy; gianluca.brando@unina.it (G.B.); ivan.spina@unina.it (I.S.)
* Correspondence: adolfo.dannier@unina.it; Tel.: +39-081-768-3233

Abstract: This paper focuses on the performance analysis of a sensorless control for a Doubly Fed Induction Generator (DFIG) in grid-connected operation for turbine-based wind generation systems. With reference to a conventional stator flux based Field Oriented Control (FOC), a full-order adaptive observer is implemented and a criterion to calculate the observer gain matrix is provided. The observer provides the estimated stator flux and an estimation of the rotor position is also obtained through the measurements of stator and rotor phase currents. Due to parameter inaccuracy, the rotor position estimation is affected by an error. As a novelty of the discussed approach, the rotor position estimation error is considered as an additional machine parameter, and an error tracking procedure is envisioned in order to track the DFIG rotor position with better accuracy. In particular, an adaptive law based on the Lyapunov theory is implemented for the tracking of the rotor position estimation error, and a current injection strategy is developed in order to ensure the necessary tracking sensitivity around zero rotor voltages. The roughly evaluated rotor position can be corrected by means of the tracked rotor position estimation error, so that the corrected rotor position is sent to the FOC for the necessary rotating coordinate transformation. An extensive experimental analysis is carried out on an 11 kW, 4 poles, 400 V/50 Hz induction machine testifying the quality of the sensorless control.

Keywords: doubly-fed induction generator; wind power system; sensorless control; full order observer; field oriented control; grid connected system

Citation: Brando, G.; Dannier, A.; Spina, I. Performance Analysis of a Full Order Sensorless Control Adaptive Observer for Doubly-Fed Induction Generator in Grid Connected Operation. *Energies* **2021**, *14*, 1254. https://doi.org/10.3390/en14051254

Academic Editor: Anibal De Almeida

Received: 1 February 2021
Accepted: 19 February 2021
Published: 25 February 2021

1. Introduction

The Doubly Fed Induction Generator (DFIG) is widely employed as a generator, especially in variable speed grid-connected wind energy applications. DFIGs guarantee robust and flexible systems, facilitating electric energy generation in a wide operating range of wind turbines [1–3].

In the grid-connected system, the aim is to maximize the conversion of mechanical input energy from the wind turbine into electric energy, ensuring the minimization of the cost of energy at the same time [4,5]. To meet this goal, the more widespread wind power generation system, for both small and large power, consists of a wind turbine [6,7], usually equipped with pitch control limits, a gearbox, and a DFIG directly connected to the AC grid on the stator side and driven through a power electronic converter on the rotor side. The rating of the power electronic is almost 25% of the rated power, allowing a speed range from nearly 50% to 120% of the rated speed [8].

It is clear that this Wind Energy Conversion System (WECS) is much more efficient than a constant speed squirrel cage induction generator system, but it obviously presents a greater complexity in the control, especially with regard to the knowledge of the rotor position [6].

The traditional control system of the doubly fed induction generator is based on stator flux oriented vector control [9]. Practically, using the rotor position it is possible

to decompose the rotor current space vector into two current components in order to decouple control of the flux and electromagnetic torque. A rotor position sensor is required to finalize the transformation of the rotor current space vector. As it is evident, the presence of these sensors on the shaft reduces the robustness of the whole system. In recent years, research has been very active in working to replace the traditional control with a sensorless one, achieving advantages in terms of system robustness, easy installation, and maintenance [10,11]. In the literature, several sensorless methods have been proposed. The different sensorless controls can be collected into the follows categories: open-loop estimation methods, closed-loop estimation methods [12,13], Kalman filter [14], high-frequency signal injections [15,16], Model Reference Adaptive System (MRAS) observers [17,18] with full or reduced order approaches [19–21], and other sensorless methods.

In the open-loop sensorless methods, the rotational speed is obtained via differentiation of the estimated slip angle [22–26]; in the MRAS, the adaptive models are all based on static flux–current relations, and the estimated speed is used as feedback in a vector control system—this approach is very sensitive to machine inductance [27]; in the other sensorless method, it is possible to include all types of sensorless control based on PLLs and similar to MRAS observers. Indeed, in these last cases, the error is driven to zero when the phase shift between the estimated vector and the reference vector is null [28,29]. Ultimately, it is possible to state that in each of these controls, the challenge is to evaluate the position of the rotor by means of an indirect method, preserving at the same time good estimation accuracy against possible parameter deviations.

The performances of the estimation of the rotor position are linked to the implemented control strategy, such as Field Oriented Control (FOC), Direct Torque Control (DTC) [30,31], and Direct Power Control (DPC) [32–34].

This paper deals with an experimental evaluation of the performance of a novel adaptive full-order observer, presented in [35], in order to assess the accuracy of the rotor position estimation by means of an FOC control scheme.

The novelty of this approach is the consideration of the rotor position estimation error as an additional machine parameter. This parameter is accurately tracked by the proposed adaptive law, assuring a good compensation of the projection error from the rotor frame to the stator frame. A prototype system was set up in order to validate the effectiveness of the proposed approach by means of an extensive measurement campaign.

This paper is organized as follows: in Section 2 a description of the system is presented, in Section 3, starting from the mathematical model in a matrix form, the proposed adaptive observer is illustrated, in Section 4 details of the adopted control scheme are highlighted and, finally, in Section 5, an analysis of the experimental results is reported.

2. Description of the System

The present work focuses on the system depicted in Figure 1. In particular, a Doubly Fed Induction Generator (DFIG) was mechanically connected to a wind turbine via a gearbox. The DFIG rotor windings were wound and equipped with slip rings. While the stator windings were directly connected to the three-phase AC grid, the rotor windings were fed through a back-to-back power converter consisting of a common DC link and two three–phase converters: a Voltage Source Inverter (VSI) to the rotor side and a Voltage Source Rectifier (VSR) to the AC grid side. Due to the presence of the bidirectional power converter, the DFIG can operate as a generator or motor in both sub-synchronous and super-synchronous modes. However, in typical applications, the converter can be rated as 25% of the nominal power of the whole system. This limits the sub-synchronous and super-synchronous modes to about 1/3 up and down of synchronous speed.

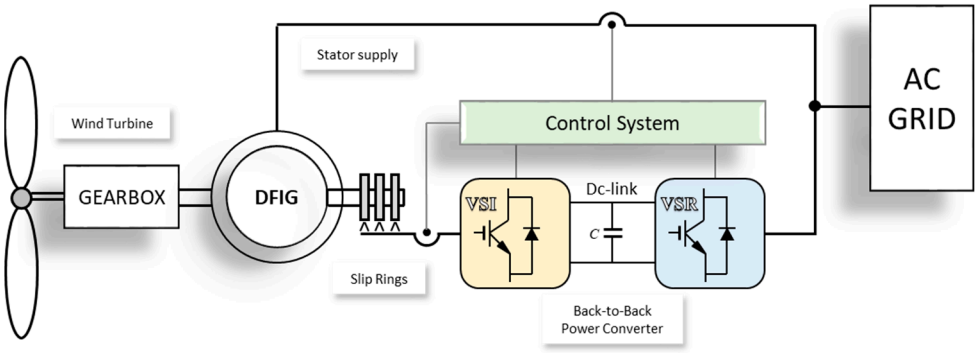

Figure 1. System block scheme.

3. Proposed Adaptive Observer

The mathematical model of the DFIG is well known and can be presented in different forms, depending on the particular choice of the state variables and the reference frame. Adopting the matrix form, the stator current and flux as state variables and the stator reference frame, the DFIG mathematical model is given by (see nomenclature at §.0):

$$\frac{\mathrm{d}}{\mathrm{d}t}\begin{bmatrix}\mathbf{i}_s\\ \mathbf{\Phi}_s\end{bmatrix} = \begin{bmatrix}A_{11} & A_{12}\\ A_{21} & A_{22}\end{bmatrix}\begin{bmatrix}\mathbf{i}_s\\ \mathbf{\Phi}_s\end{bmatrix} + \begin{bmatrix}B_1\\ B_2\end{bmatrix}[\mathbf{v}_s] + \begin{bmatrix}C_1\\ C_2\end{bmatrix}[\mathbf{v}_r] \tag{1}$$

It is worth noting that by imposing $\mathbf{v}_r = 0$ in Equation (1), the mathematical model of a traditional induction machine (with short-circuited rotor windings) is obtained.

In Equation (1), the state variables, the inputs, and the outputs are space vectors. By consequence, all the corresponding matrix elements are complex numbers. In particular

$$\begin{cases} A_{11} = -\left(\frac{R_s}{L_{s,eq}} + f_{r,eq}\right) + jp\omega_r \\ A_{12} = \frac{\sigma f_{r,eq}}{L_{s,eq}} - j\frac{p\omega_r}{L_{s,eq}} \\ A_{21} = -R_s \\ A_{22} = 0 \end{cases} \quad \begin{cases} B_1 = \frac{1}{L_{s,eq}} \\ B_2 = 1 \end{cases} \quad \begin{cases} C_1 = -\frac{B_1}{\mu_r} \\ C_2 = 0 \end{cases} \tag{2}$$

where:

$$\mu_r = \frac{L_m}{L_r};\ \sigma = (1 - \mu_s\mu_r);\ L_{s,eq} = \sigma L_s;\ f_{r,eq} = \frac{R_r}{L_{r,eq}} \tag{3}$$

with $\mu_s = L_m/L_r$ and $L_{r,eq} = \sigma L_r$.

It is possible to derive the space vector of the rotor current from the definition of the stator flux ($\mathbf{\Phi}_s = L_s\mathbf{i}_s + L_m\mathbf{i}_r$):

$$\mathbf{i}_r = \frac{\mathbf{\Phi}_s}{L_m} - \frac{L_s}{L_m}\mathbf{i}_s \tag{4}$$

The following full-order Lueberger observer can be defined based on the DFIG mathematical model (Equation (1)):

$$\frac{\mathrm{d}}{\mathrm{d}t}\begin{bmatrix}\hat{\mathbf{i}}_s\\ \hat{\mathbf{\Phi}}_s\end{bmatrix} = A\begin{bmatrix}\hat{\mathbf{i}}_s\\ \hat{\mathbf{\Phi}}_s\end{bmatrix} + B[\mathbf{v}_s] + C[\mathbf{v}_r] + \begin{bmatrix}G_1\\ G_2\end{bmatrix}[\mathbf{i}_s - \hat{\mathbf{i}}_s] \tag{5}$$

The elements G_1 and G_2 of the observer matrix should be designed with reference to the observer state matrix A_O:

$$A_O = \begin{bmatrix}A_{11} - G_1 & A_{12}\\ A_{21} - G_2 & A_{22}\end{bmatrix} \tag{6}$$

having eigenvalues $p_{O,1}$ and $p_{O,2}$. It should be noted that the above equations relate to a proportional type Lueberger observer. Other more complex architectures (such as proportional–integral and modified integral [36]) may lead to an overall improved noise

rejection. However, the proportional type allows for a relatively simple selection of the observer gains. In particular, the observer gains should be selected such as that the error $\mathbf{i}_s - \hat{\mathbf{i}}_s$ quickly converges to zero. In other words, the observer dynamic must be faster than that of the DFIG in all operating conditions and, in particular, for any value of the rotational speed. The faster DFIG dynamic is linked to the DFIG high-frequency pole $p_{D,HF}$ at zero speed. Thus, by introducing an overall observer gain $K_G > 1$, the two observer poles that $p_{O,1}$ and $p_{O,2}$ can be fixed proportional to $p_{D,HF}$ through K_G. Considering that a good approximation by excess of the effective $p_{D,HF}$ value is:

$$p_{D,HF} \cong -\left(\frac{R_s}{L_{s,eq}} + f_{r,eq}\right) \tag{7}$$

the eigenvalues $p_{O,1}$, $p_{O,2}$ can be fixed as:

$$p_{O,1} = p_{O,2} = p_O = -K_G\left(\frac{R_s}{L_{s,eq}} + f_{r,eq}\right) \tag{8}$$

where K_G is the overall observer gain.

In order to preserve system stability, an optimal value for K_G should be eventually fixed by trials on the real system, depending on the measurement equipment and noise; K_G values are typically chosen between 2 and 5. Hence, the elements G_1 and G_2 of the observer matrix are given by:

$$\begin{cases} G_1 = A_{11} - 2p_O \\ G_2 = A_{21} + p_O^2/A_{12} \end{cases} \tag{9}$$

In the dynamic system (Equation (5)), the space vectors $\mathbf{v}_r$,$\mathbf{v}_s$ and $\mathbf{i}_s$ represent inputs. In particular, while $\mathbf{v}_s$ and $\mathbf{i}_s$ can be simply measured by voltage and current transducers, knowledge of $\mathbf{v}_r$ would require an additional rotor position sensor. Indeed, $\mathbf{v}_r$ is defined by a rotational transformation of the actual space vector voltage $\mathbf{v}_r^{(r)}$ provided by the rotor power converter through the electrical rotor position ϑ_e:

$$\mathbf{v}_r = \mathbf{v}_r^{(r)} e^{j\vartheta_e} \tag{10}$$

where

$$\vartheta_e = p\vartheta_r \tag{11}$$

with ϑ_r represents the mechanical rotor position and p the number of pole pairs.

On the other hand, in the context of a sensorless control, the observer outputs can be exploited in order to estimate the rotor position and, consequently, the space vector of the rotor voltage in the stator reference frame $\mathbf{v}_r$, without the use of an additional position sensor.

The rotor position can be estimated considering that Relation (10) also applies to the rotor current space vector in the two reference frames:

$$\mathbf{i}_r = \mathbf{i}_r^{(r)} e^{j\vartheta_e} \tag{12}$$

where, naturally, $\mathbf{i}_r^{(r)}$ is the rotor current space vector provided by the power converter and $\mathbf{i}_r$ is the rotor current space vector in the stator frame.

While the quantity $\mathbf{i}_r^{(r)}$ is directly measurable at the converter terminals, an estimated version of $\mathbf{i}_r$ can be calculated as per Equation (4) by substituting the actual flux $\mathbf{\Phi}_s$ with the estimated one $\hat{\mathbf{\Phi}}_s$:

$$\hat{\mathbf{i}}_r = \frac{\hat{\mathbf{\Phi}}_s}{L_m} - \frac{L_s}{L_m}\mathbf{i}_s \tag{13}$$

Once $\mathbf{i}_r^{(r)}$ and $\hat{\mathbf{i}}_r$ are known, the rotor electrical position can be derived as:

$$e^{j\hat{\vartheta}_e} = \frac{\hat{\mathbf{i}}_r}{\mathbf{i}_r^{(r)}} \Rightarrow \hat{\vartheta}_e = \arg\left(\hat{\mathbf{\Phi}}_s - L_s\mathbf{i}_s\right) - \arg\left(\mathbf{i}_r^{(r)}\right) \tag{14}$$

Hence, $\mathbf{v}_r$ can be calculated as per Equation (10).

The knowledge of $\hat{\vartheta}_e$ also allows for the computation of the rotor speed via the numerical time derivative. In order to dampen the oscillations resulting from the time derivative computation, the calculation of the rotor speed should be processed by a properly sized Low Pass Filter (LPF):

$$\hat{\omega}_r = \frac{1}{p}\Im\left(\frac{d\hat{\theta}}{dt}\right) \tag{15}$$

where $\Im$ denotes the functional associated to the LPF.

As expected, knowledge of machine parameter values plays an important role in the described estimation procedure. However, the machine parameters cannot be known with absolute precision, and only their estimated values can actually be used in the previous equations. In particular, the symbols A, B, C, $\mathbf{v}_r$ and L_s appearing in Equations (5), (10), and (14) should formally be replaced with $\hat{A}$, $\hat{B}$, $\hat{C}$, $\hat{\mathbf{v}}_r$ and $\hat{L}_s$, this last representing their estimated versions. As a consequence of the possible parameter deviations, the rotor position estimation $\hat{\vartheta}_e$ will be affected by inaccuracy.

Let us define $\Delta\vartheta_e$ as the rotor position estimation error:

$$\Delta\vartheta_e = \vartheta_e - \hat{\vartheta}_e \tag{16}$$

According to Definition (16), the actual rotor position ϑ_e can be expressed as $\hat{\vartheta}_e + \Delta\vartheta_e$. Hence, the actual rotor voltage $\mathbf{v}_r$ can be written as:

$$\mathbf{v}_r = \mathbf{v}_r^{(r)} e^{j(\hat{\vartheta}_e + \Delta\vartheta_e)} = \mathbf{v}_r^{(r)} e^{j\hat{\vartheta}_e} e^{j\Delta\vartheta_e} = \hat{\mathbf{v}}_r e^{j\Delta\vartheta_e} \tag{17}$$

where the quantity $\mathbf{v}_r^{(r)} e^{j\hat{\vartheta}_e}$ corresponds to $\hat{\mathbf{v}}_r$: the estimated version of the rotor voltage.

Equation (17) clarifies that the estimated rotor voltage $\hat{\mathbf{v}}_r$ does not correspond to the actual rotor voltage $\mathbf{v}_r$ due the projection error $e^{j\Delta\vartheta_e}$. At the same time, this suggests that the projection error could be compensated if a $\Delta\vartheta_e$ tacking procedure is conceived.

Let us denote the tracking procedure output with $\Delta\hat{\vartheta}_e$. i.e., $\Delta\hat{\vartheta}_e$ is the estimation of the actual $\Delta\vartheta_e$ value. For small $\Delta\hat{\vartheta}_e$ values, the following approximation can be assumed:

$$e^{j\Delta\hat{\vartheta}_e} = \cos\Delta\hat{\vartheta}_e + j\sin\Delta\hat{\vartheta}_e \cong 1 + j\Delta\hat{\vartheta}_e \tag{18}$$

In light of the previous consideration on the parameter deviations, and considering Equation (17) with approximation (18), the Luemberger observer (Equation (5)) can now be re-written:

$$\frac{\mathrm{d}}{\mathrm{d}t}\begin{bmatrix} \hat{\mathbf{i}}_s \\ \hat{\mathbf{\Phi}}_s \end{bmatrix} = \hat{A}\begin{bmatrix} \hat{\mathbf{i}}_s \\ \hat{\mathbf{\Phi}}_s \end{bmatrix} + \hat{B}[\mathbf{v}_s] + \hat{C}\left(1 + j\Delta\hat{\vartheta}_e\right)[\hat{\mathbf{v}}_r] + G[\mathbf{e}] \tag{19}$$

where $G = \begin{bmatrix} G_1 & G_2 \end{bmatrix}^T$ and $\mathbf{e} = \mathbf{i}_s - \hat{\mathbf{i}}_s$.

The quantity $\Delta\hat{\vartheta}_e$ in Equation (19) can be regarded as an additional machine parameter, and its value can be estimated by the following adaptive law based on the Lyapunov theory:

$$\Delta\hat{\vartheta}_e = K_{\Delta\vartheta}\int_0^t \left(\hat{v}_{ry}e_x - \hat{v}_{rx}e_y\right)dt + \Delta\hat{\vartheta}_{e0} \tag{20}$$

where $K_{\Delta\vartheta}$ is a not negative number.

The model (Equation (19)) and the adaptive law (Equation (20)), together with the Relations (14) and (15), define the proposed adaptive observer, which provides the estima-

tion of rotor speed $\hat{\omega}_r$ and position $\hat{\vartheta}_e$. Moreover, the proposed technique is robust against possible machine parameter uncertainties and is capable of tracking the rotor position estimation error $\Delta\hat{\vartheta}_e$.

4. Control Scheme

In the control scheme depicted in Figure 2, the proposed sensorless adaptive observer provides the necessary rotational transformation angle and the rotor speed value for a traditional stator flux Field Oriented Control (FOC). In particular x, y represent the stator reference frame axis; α, β refer to the rotor reference frame axis; and d, q represents the rotating reference frame aligned with the stator flux $\mathbf{\Phi}_s$.

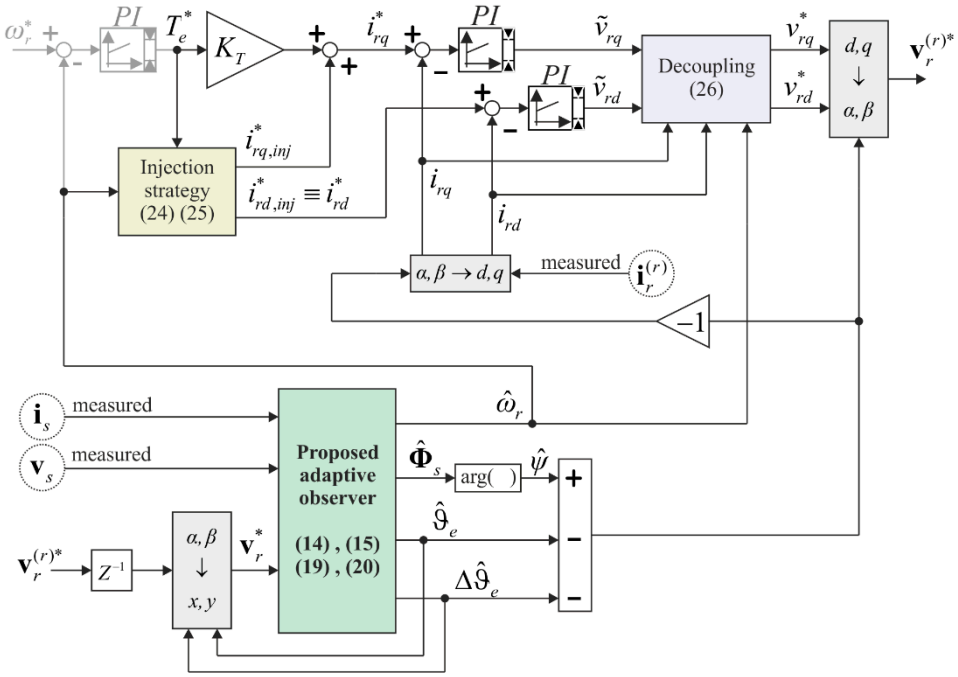

Figure 2. Control diagram.

Since the observer model has been written into the stator reference frame, its inputs ($\mathbf{v}_s$, $\mathbf{i}_s$ and $\mathbf{v}_r$) are referred to as x, y coordinates. In particular, while the first two inputs are measured directly on the stator side connected to the AC grid, the third input needs to be transformed from α, β to x, y coordinates. Indeed, the quantity $\mathbf{v}_r^{*(r)} = v_{r\alpha}^* + jv_{r\beta}^*$, representing the reference voltage for the VSI, is transformed into x, y coordinates by the angle $\hat{\vartheta}_e + \Delta\hat{\vartheta}_e$. In this way, the projection error is compensated by the position estimation error.

The adaptive observer outputs are the estimation of rotor speed $\hat{\omega}_r$, position $\hat{\vartheta}_e$, the rotor position estimation error $\Delta\hat{\vartheta}_e$ and the stator flux space vector $\mathbf{\Phi}_s$. From this last output, it is possible to calculate the angle of the stator flux $\hat{\psi}$:

$$\hat{\psi} = \arg\left(\hat{\mathbf{\Phi}}_s\right) \tag{21}$$

The necessary transformation from α, β to x, y coordinates can thus be operated by the angle $\hat{\vartheta}_e + \Delta\hat{\vartheta}_e - \hat{\psi}$:

$$\mathbf{i}_r^{(\Phi)} = \mathbf{i}_r^{(r)} e^{j\left(\hat{\vartheta}_e + \Delta\hat{\vartheta}_e\right)} e^{-j\hat{\psi}} = i_{rd} + ji_{rq} \tag{22}$$

where $\mathbf{i}_r^{(r)}$ is the rotor current space vector, measurable in α, β coordinates.

As per the traditional FOC scheme, the obtained components i_{rd},i_{rq} are processed by two PI controllers driven by the errors computed with respect to the correspondent

reference quantities i^*_{rd},i^*_{rq}. In particular, while i^*_{rq} is set proportional to the reference torque T^*_e by the torque constant K_T, i^*_{rd} should be set equal to zero. However, it must be considered that the tracking of ϑ_e and $\Delta\vartheta_e$ could prove ineffective during very low torque operating conditions where both current components move toward zero. For this reason, an injection strategy has been implemented:

$$\begin{cases} i^*_{rd} = i^*_{rd,inj} \\ i^*_{rq} = K_T T^*_e + i^*_{rq,inj} \end{cases} \tag{23}$$

where:

$$\begin{cases} i^*_{rd,inj} = \lambda_d A_{inj} \cos(2\pi f_{inj} t) \\ i^*_{rq,inj} = \lambda_q A_{inj} \cos(2\pi f_{inj} t) \end{cases} \tag{24}$$

A_{inj} and f_{inj} are the amplitude and the frequency of the injected current components. Activation and deactivation of the injection are operated through λ_d and λ_q, which can assume either 0 or 1 values. The q injection is activated if the required torque is too small. The d injection is activated if the required torque is too small or if the slip angular frequency is too small. Fixing $\Delta T_{e,inj}$ and $\Delta\omega_{inj}$ as threshold values, respectively, for the required torque and the slip angular frequency, λ_d and λ_q can be expressed as (in C language style):

$$\begin{cases} \lambda_d = |p\omega_r - \omega| < \Delta\omega_{inj} \;||\; |T^*_e| < \Delta T_{e,inj} \\ \lambda_q = |T^*_e| < \Delta T_{e,inj} \end{cases} \tag{25}$$

The converter space vector reference voltage components v^*_{rd}, v^*_{rq} are obtained by compensating the current PI regulator outputs $\widetilde{v}_{rd}$, $\widetilde{v}_{rq}$ through the decoupling action:

$$\begin{cases} v^*_{rd} = \widetilde{v}_{rd} - \hat{\omega}_\sigma L_{s,eq} i_{rq} \\ v^*_{rq} = \widetilde{v}_{rq} + \hat{\omega}_\sigma L_{s,eq} i_{rd} + \hat{\omega}_\sigma \Phi_{s,R} \end{cases} \tag{26}$$

with $\hat{\omega}_\sigma = \omega - p\hat{\omega}_r$ being the estimated rotor slip angular frequency, and $\Phi_{s,R}$ being the rated stator flux.

Finally, the obtained space vector $v^*_{rd} + jv^*_{rq} = \mathbf{v}^{*(\Phi)}_r$ is transformed from d, q to α, β coordinates by the angle $\hat{\psi} - \hat{\vartheta}_e - \Delta\hat{\vartheta}_e$:

$$\mathbf{v}^{*(r)}_r = \mathbf{v}^{*(\Phi)}_r e^{-j(\hat{\vartheta}_e + \Delta\hat{\vartheta}_e)} e^{j\hat{\psi}} = v^*_{r\alpha} + jv^*_{r\beta} \tag{27}$$

The α, β components of Equation (27) can be modulated as per a Space Vector Modulation (SVM) in order to drive the VSI at the rotor side. Naturally, as mentioned above, $\mathbf{v}^{*(r)}_r$ is also sent back and, through a unit time delay, constitutes a closed loop for the proposed adaptive law.

5. Experimental Results

The proposed control strategy was validated experimentally by mechanically connecting a three-phase wound rotor, 11 kW, 4 poles, 400 V/50 Hz induction machine to a 27 kW DC machine acting as a prime motor. Both the electric machines were driven by power converters based on Semikron IGBT modules, while the system control was implemented on *dSpace 1103* hardware whose digital outputs were properly routed to the IGBT drivers' inputs. The whole experimental setup is shown in Figure 3. In order to evaluate the sensorless estimation errors, a 4000 pulse/round incremental encoder mechanically connected to the DFIG was used to determine the rotor speed and position.

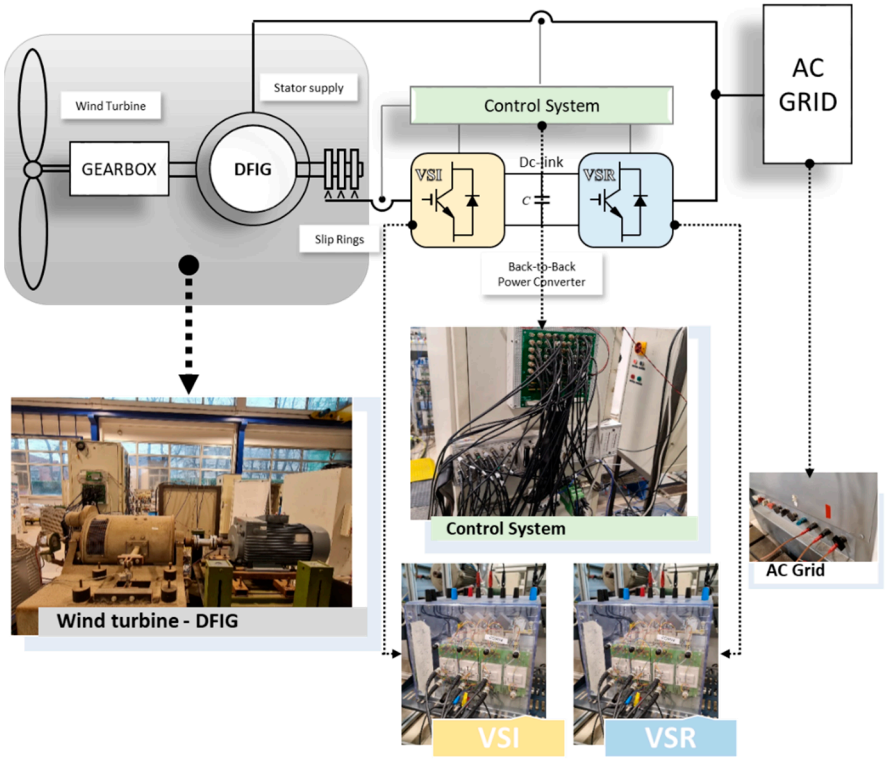

Figure 3. Experimental setup.

The motor parameters used to build the observer matrix were estimated by means of standard blocked rotor/no-load IEEE 112 tests executed on the DFIG. Since no additional parameter tuning was carried out, the experimental results also highlight the robustness of the adaptive observer with respect to substantial parameter deviations in the characterization of the induction machine. Indeed, standard IEEE 112 tests are affected by non-negligible errors, especially when compared to more advanced off-line estimation methods [37]. This approach allows us, therefore, to portray the improved accuracy in rotor position estimation granted by the adaptive observer in comparison to a standard observer.

To validate the effectiveness of the conceived adaptation law both at different speed values and different torque values, the following test was performed:

(a) Initially, a startup procedure (which is not shown) takes the system to the test initial condition, where the rotor speed is set to 70% of the DFIG synchronous speed and the DFIG reference torque is set to 50% of its rated value. Steady state condition is reached at $t = 0$.
(b) After one second of steady state condition, (at $t = 1$) the DFIG reference torque is set to the full rated value and again to half its rated value after one second (at $t = 2$).
(c) At $t = 3$ the reference speed is changed to the DFIG synchronous speed. To achieve a quasi-stationary transition which allows us to check the system response in the whole speed range, the reference speed was processed by a rate limiter filter. Consequently, the speed reached the new reference value through a linear behavior in around 2.2 s.
(d) The two-step torque variation of point (b) was repeated.
(e) The reference speed was changed to 130% of the DFIG synchronous speed.
(f) The two-step torque variation of point (b) was repeated, and the test was concluded.

The experimental results of the whole test are shown in Figure 4 (rotor speed), Figure 5 (rotor axes currents), and Figure 6 (rotor electric angle estimation error). From Figure 4, where both the measured and estimated rotor speed are plotted, it can be deduced that the DFIG observer was able to effectively track the real system speed with a negligible error, which stayed always under 0.5%. Naturally, the observable speed over- and under-

shoots are linked to the corresponding step variations of the DFIG reference torque. From Figure 5, where both the reference and actual rotor axes currents are plotted, it can be deduced that the control system (driven by the estimated values of the rotor speed and position) was able to effectively drive the rotor currents in the whole speed range. It should be pointed out that the ripples in the rotor axis current are visible only around the DFIG synchronous speed. This is indeed the result of the frequency injection in the rotor currents, which is used to keep the adaptation law sensible to the rotor voltage projection error when the rotor voltages become too small (in this instance, when the DFIG was around the synchronous operation mode). Finally, Figure 6 shows the rotor position error obtained with the proposed adaptation law versus that which would affect the observer when the adaptation law was not engaged. It can be deduced that the performance of the observer is appreciably improved: while the position error was kept between −5 degrees and 8 degrees with the adaptation law, it varied between 10 degrees and 20 degrees when the position error was not compensated. The maximum improvement can be noted at the low speed, where the error is 3 degrees, versus 17–20 degrees at the high speed.

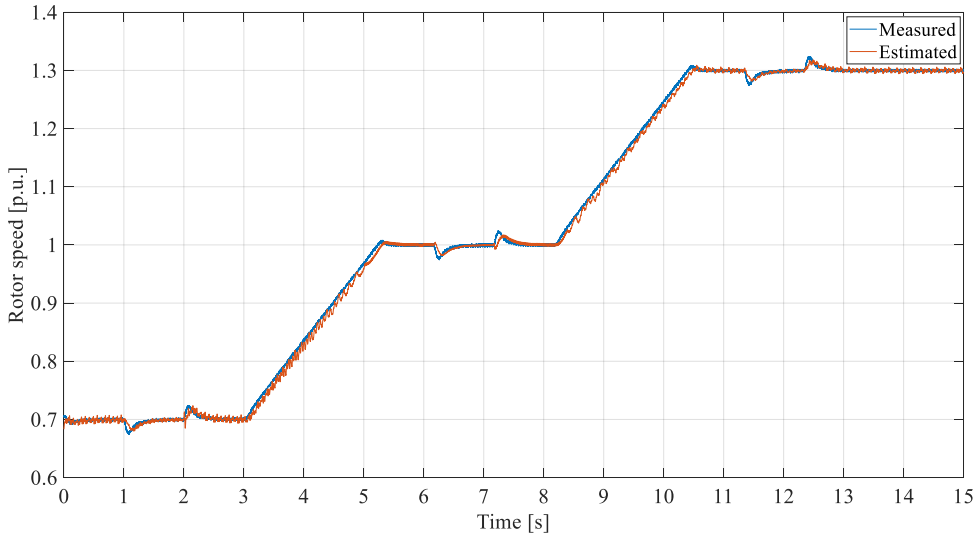

Figure 4. Behavior of the estimated and actual rotor speed in the whole test.

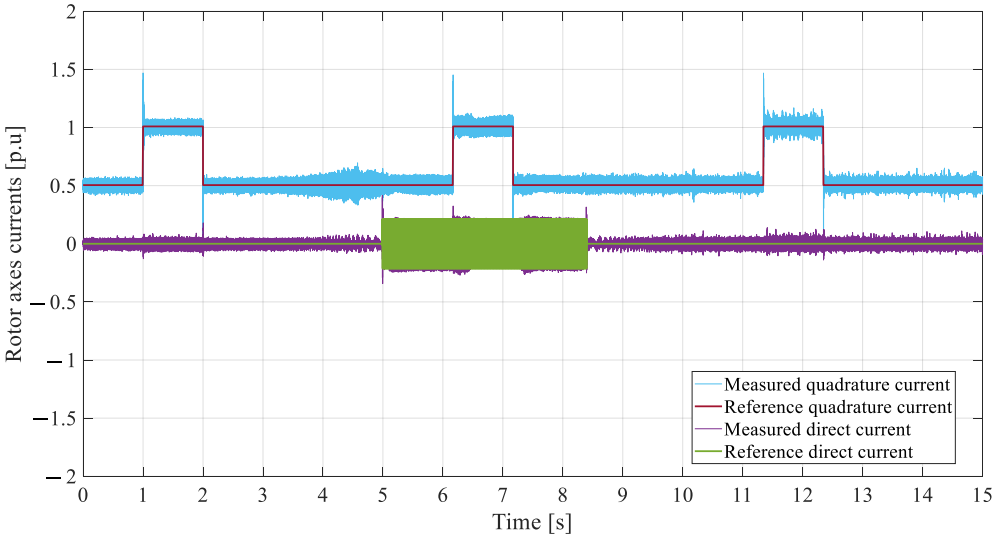

Figure 5. Behavior of the reference and actual rotor axes currents in the whole test.

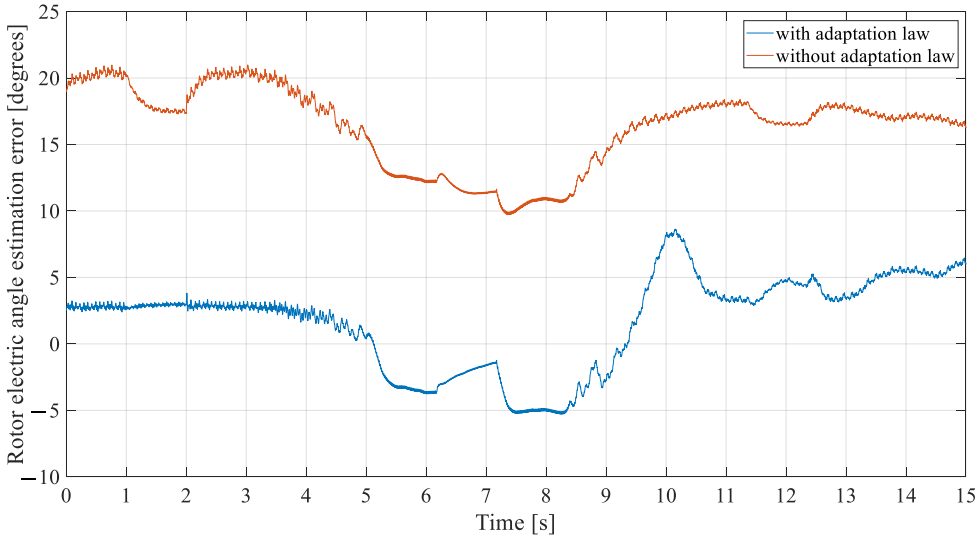

Figure 6. Behavior of the position estimation error with/without adaptation law in the whole test.

Figure 7 shows the behaviors of the first and second phase stator currents (green and violet lines) versus the corresponding rotor currents (blue and red lines) when the rotor speed was equal to 130% of the synchronous speed and the reference torque was set to 100% of the rated value. As expected, while the stator currents oscillated at the grid frequency (50 Hz), the frequency of the rotor currents were linked to the actual rotor speed. Given the value of the rotor speed, the resulting frequency was 15 Hz—this value is coherent with the difference between the synchronous speed and the actual one. It can also be noted that the first phase rotor current lagged after the second phase current—this is also expected since the DFIG was working with a rotor speed higher than the synchronous one.

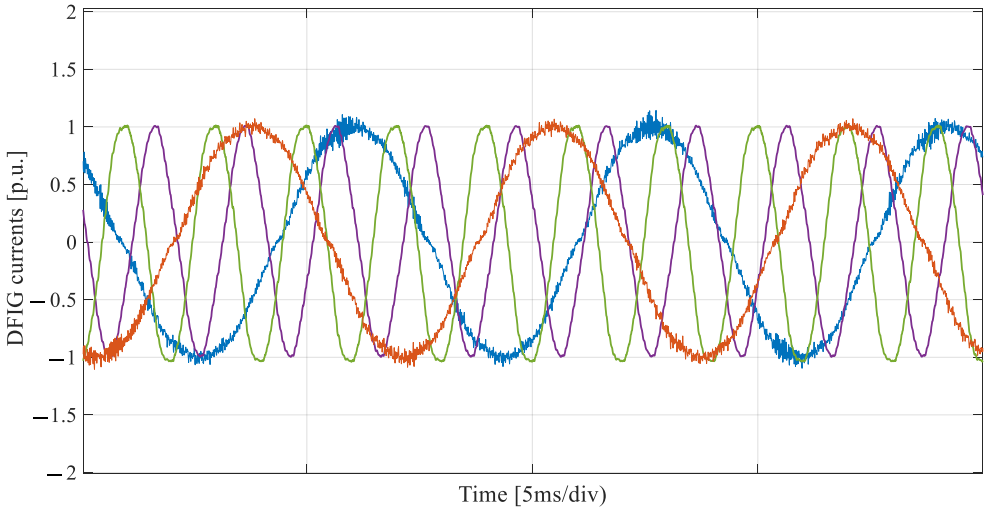

Figure 7. Behavior of the DFIG stator and rotor currents at the rated torque in the high speed region.

6. Conclusions

The aim of this paper is to experimentally evaluate the performance of a novel adaptive full-order observer in order to assess the accuracy of rotor position estimation by means of a Field Oriented Control (FOC) scheme for a Doubly Fed Induction generator (DFIG).

In particular, the work demonstrates that the rotor position evaluated by the observer estimated flux can be affected by significant errors due to parameter inaccuracies. The novelty of the proposed approach is linked to the fact that the rotor position estimation error is considered as an additional machine parameter. Thus, an adaptive law based on the Lyapunov theory was proposed for the tracking of the rotor position estimation error and,

additionally, a current injection strategy was developed in order to ensure the necessary tracking sensitivity around zero rotor voltages. The roughly evaluated rotor position was corrected by means of the tracked rotor position estimation error so that the corrected rotor position was sent to the FOC for the necessary rotating coordinate transformation.

The proposed technique was tested experimentally on an 11 kW DFIG prototype moved by a 27 kW DC machine acting as the prime motor. The experimental results testify to the quality of the sensorless control, which is able to effectively track the real system speed with a negligible error (< 0.5%) in the range of 60–130% of the rated speed value. Moreover, the proposed adaptive law clearly improved observer performance by significantly reducing the rotor position estimation error from 17–20 degrees to 3 degrees in the best case.

Future work will focus on the analytical analysis of the stability of the conceived adaptive observer and on its robustness with respect to parameter variations and electric grid and mechanical perturbances, such as negative voltage sequences or rotor eccentricity.

Author Contributions: G.B. formalized the control algorithm and wrote the relevant section, I.S. implemented the control algorithm on the real time controller and wrote the relevant section, A.D. supervised the experimental tests, wrote the other sections and edited the whole manuscript. All authors have read and agreed to the published version of the manuscript.

Funding: This research received no external funding.

Institutional Review Board Statement: Not applicable.

Informed Consent Statement: Not applicable.

Conflicts of Interest: The authors declare no conflict of interest.

Abbreviations

$\mathbf{i}_s / \mathbf{i}_r$	Space vector of the stator/rotor current
$L_{\sigma s} / L_{\sigma r}$	Stator/rotor leakage inductance
L_m	Air-gap linkage inductance
L_s	Stator inductance $L_s = L_{\sigma s} + L_m$
L_r	Rotor inductance $L_r = L_{\sigma r} + L_m$
R_s / R_r	Stator/rotor resistance
$\mathbf{v}_s / \mathbf{v}_r$	Space vector of the stator/rotor voltage
$\vartheta_r / \vartheta_e$	Mechanical/electrical rotor position
$\mathbf{\Phi}_s / \mathbf{\Phi}_r$	Space vector of the stator/rotor flux
ω_r / ω	Rotor angular speed/angular frequency
$\hat{}$	Superscript to indicate estimated quantity
$*$	Superscript to indicate reference quantity
(r)	Superscript to indicate rotor reference frame

References

1. Carrasco, J.; Franquelo, L.; Bialasiewicz, J.; Galvan, E.; PortilloGuisado, R.; Prats, M.; Leon, J.; Moreno-Alfonso, N. Power-Electronic Systems for the Grid Integration of Renewable Energy Sources: A Survey. *IEEE Trans. Ind. Electron.* **2006**, *53*, 1002–1016. [CrossRef]
2. Cardenas, R.; Pena, R.; Alepuz, S.; Asher, G. Overview of Control Systems for the Operation of DFIGs in Wind Energy Applications. *IEEE Trans. Ind. Electron.* **2013**, *60*, 2776–2798. [CrossRef]
3. Li, C.; Hang, Z.; Zhang, H.; Guo, Q.; Zhu, Y.; Terzija, V. Evaluation of DFIGs' Primary Frequency Regulation Capability for Power Systems with High Penetration of Wind Power. *Energies* **2020**, *13*, 6178. [CrossRef]
4. Qiao, W.; Zhou, W.; Aller, J.; Harley, R. Wind Speed Estimation Based Sensorless Output Maximization Control for a Wind Turbine Driving a DFIG. *IEEE Trans. Power Electron.* **2008**, *23*, 1156–1169. [CrossRef]
5. Baran, J.; Jąderko, A. An MPPT Control of a PMSG-Based WECS with Disturbance Compensation and Wind Speed Estimation. *Energies* **2020**, *13*, 6344. [CrossRef]
6. Polinder, H.; Ferreira, J.A.; Jensen, B.B.; Abrahamsen, A.B.; Atallah, K.; McMahon, R.A. Trends in Wind Turbine Generator Systems. *IEEE J. Emerg. Sel. Top. Power Electron.* **2013**, *1*, 174–185. [CrossRef]

7. Guo, J.; Lei, L. Flow Characteristics of a Straight-Bladed Vertical Axis Wind Turbine with Inclined Pitch Axes. *Energies* **2020**, *13*, 6281. [CrossRef]
8. Muller, S.; Deicke, M.; De Doncker, R.W. Doubly fed induction generator systems for wind turbines. *IEEE Ind. Appl. Mag.* **2002**, *8*, 26–33. [CrossRef]
9. Tapia, A.; Tapia, G.; Ostolaza, J.X.; Saenz, J.R. Modeling and control of a wind turbine driven doubly fed induction generator. *IEEE Trans. Energy Convers.* **2003**, *18*, 194–204. [CrossRef]
10. Holtz, J. Sensorless control of induction motor drives. *Proc. IEEE* **2002**, *90*, 1359–1394. [CrossRef]
11. Holtz, J. Sensorless Control of Induction Machines—With or Without Signal Injection? *IEEE Trans. Ind. Electron.* **2006**, *53*, 7–30. [CrossRef]
12. Malakar, M.K.; Tripathy, P.; Krishnaswamy, S. A predictor-corrector based rotor slip-position estimation technique for a DFIG. In Proceedings of the 2017 7th International Conference on Power Systems (ICPS), Pune, India, 21–23 December 2017; pp. 424–429.
13. Soares, E.L.; Rocha, F.V.; De Siqueira, L.M.S.; Rocha, N. Sensorless Rotor Position Detection of Doubly-Fed Induction Generators for Wind Energy Applications. In Proceedings of the 2018 13th IEEE International Conference on Industry Applications (INDUSCON), São Paulo, Brazil, 12–14 November 2018; pp. 1045–1050.
14. Abdelrahem, M.; Hackl, C.; Kennel, R. Sensorless control of doubly-fed induction generators in variable-speed wind tur-bine systems. In Proceedings of the 2015 International Conference on Clean Electrical Power (ICCEP), Taormina, Italy, 16–18 June 2015; pp. 406–413.
15. Reigosa, D.D.; Briz, F.; Charro, C.B.; di Gioia, A.; García, P.; Guerrero, J.M. Sensorless Control of Doubly Fed Induc-tion Generators Based on Rotor High-Frequency Signal Injection. In Proceedings of the 2012 IEEE Energy Conversion Congress and Exposition (ECCE), Raleigh, NC, USA, 15–20 September 2012; pp. 2268–2275.
16. Xu, L.; Inoa, E.; Liu, Y.; Guan, B. A New High-Frequency Injection Method for Sensorless Control of Doubly Fed Induc-tion Machines. *IEEE Trans. Ind. Appl.* **2012**, *48*, 1556–1564. [CrossRef]
17. Cárdenas, R.; Peña, R.; Proboste, J.; Asher, G.; Clare, J.; Wheeler, P. MRAS observers for sensorless control of doubly-fed induction generators. In Proceedings of the 4th IET Conference on Power Electronics, Machines and Drives, York, UK, 2–4 April 2008; pp. 568–572.
18. Pattnaik, M.; Kastha, D. Adaptive speed observer for a stand-alone doubly fed induction generator feeding nonlinear and unbalanced loads. In Proceedings of the 2013 IEEE Power & Energy Society General Meeting, Vancouver, BC, Canada, 21–25 July 2013.
19. Bhattarai, R.; Gurung, N.; Thakallapelli, A.; Kamalasadan, S. Reduced-Order State Observer-Based Feedback Control Methodolo-gies for Doubly Fed Induction Machine. *IEEE Trans. Ind. Appl.* **2018**, *54*, 2845–2856. [CrossRef]
20. Forchetti, D.G.; Garcia, G.O.; Valla, M.I. Adaptive Observer for Sensorless Control of Stand-Alone Doubly Fed Induction Generator. *IEEE Trans. Ind. Electron.* **2009**, *56*, 4174–4180. [CrossRef]
21. Yang, S.; Ajjarapu, V. A Speed-Adaptive Reduced-Order Observer for Sensorless Vector Control of Doubly Fed Induc-tion Generator-Based Variable-Speed Wind Turbines. *IEEE Trans. Energy Convers.* **2010**, *25*, 891–900. [CrossRef]
22. Abolhassani, M.; Niazi, P.; Toliyat, H.; Enjeti, P. A sensorless integrated doubly-fed electric alternator/active filter (IDEA) for variable speed wind energy system. In Proceedings of the 38th IAS Annual Meeting on Conference Record of the Industry Applications Conference, Salt Lake City, UT, USA, 12–16 October 2003; pp. 507–514.
23. Datta, R.; Ranganathan, V.T. A simple position-sensorless algorithm for rotor-side field-oriented control of wound-rotor induction machine. *IEEE Trans. Ind. Electron.* **2001**, *48*, 786–793. [CrossRef]
24. Morel, L.; Godfroid, H.; Mirzaian, A.; Kauffmann, J. Double-fed induction machine: Converter optimisation and field oriented control without position sensor. *IEE Proc. Electr. Power Appl.* **1998**, *145*, 360. [CrossRef]
25. Krzeminski, Z. Sensorless control of a double-fed machine for wind power generators. In Proceedings of the Power Conversion Conference, Osaka, Croatia, 2–5 April 2002. [CrossRef]
26. Hopfensperger, B.; Atkinson, D.; Lakin, R. Stator-flux-oriented control of a doubly-fed induction machine: With and without position encoder. *IEE Proc. Electr. Power Appl.* **2000**, *147*, 241–250. [CrossRef]
27. Schauder, C. Adaptive speed identification for vector control of induction motors without rotational transducers. *IEEE Trans. Ind. Appl.* **1992**, *28*, 1054–1061. [CrossRef]
28. Cardenas, R.; Pena, R.; Clare, J.; Asher, G.; Proboste, J. MRAS observers for sensorless control of doubly-fed induction generators. *IEEE Trans. Power Electron.* **2008**, *23*, 1075–1084. [CrossRef]
29. Castelli-Dezza, F.; Foglia, G.; Iacchetti, M.F.; Perini, R. An MRAS observer for sensorless DFIM drives with direct estima-tion of the torque and flux rotor current components. *IEEE Trans. Power Electron.* **2012**, *27*, 2576–2584. [CrossRef]
30. Mondal, S.; Kastha, D. Improved Direct Torque and Reactive Power Control of a Matrix-Converter-Fed Grid-Connected Doubly Fed Induction Generator. *IEEE Trans. Ind. Electron.* **2015**, *62*, 7590–7598. [CrossRef]
31. Arbi, J.; Ghorbal, M.J.; Slama-Belkhodja, I.; Charaabi, L. Direct Virtual Torque Control for Doubly Fed Induction Genera-tor Grid Connection. *IEEE Trans. Ind. Electron.* **2009**, *56*, 4163–4173. [CrossRef]
32. Hu, J.; Zhu, J.; Zhang, Y.; Platt, G.; Ma, Q.; Dorrell, D.G. Predictive Direct Virtual Torque and Power Control of Doubly Fed Induction Generators for Fast and Smooth Grid Synchronization and Flexible Power Regulation. *IEEE Trans. Power Electron.* **2012**, *28*, 3182–3194. [CrossRef]

33. Amiri, N.; Madani, S.M.; Lipo, T.A.; Zarchi, H.A. An Improved Direct Decoupled Power Control of Doubly Fed Induc-tion Machine Without Rotor Position Sensor and With Robustness to Parameter Variation. *IEEE Trans. Energy Convers.* **2012**, *27*, 873–884. [CrossRef]
34. Abad, G.; Rodriguez, M. Ángel; Poza, J. Three-Level NPC Converter-Based Predictive Direct Power Control of the Doubly Fed Induction Machine at Low Constant Switching Frequency. *IEEE Trans. Ind. Electron.* **2008**, *55*, 4417–4429. [CrossRef]
35. Brando, G.; Dannier, A.; Spina, I. A Full Order Sensorless Control Adaptive Observer for Doubly-Fed Induction Generator. In Proceedings of the 2019 International Conference on Clean Electrical Power (ICCEP), Otranto, Italy, 2–4 July 2019; pp. 464–469.
36. Białoń, T.; Pasko, M.; Niestrój, R. Developing Induction Motor State Observers with Increased Robustness. *Energies* **2020**, *13*, 5487. [CrossRef]
37. Wu, R.-C.; Tseng, Y.-W.; Chen, C.-Y. Estimating Parameters of the Induction Machine by the Polynomial Regression. *Appl. Sci.* **2018**, *8*, 1073. [CrossRef]